

# ETA-IK: Execution-Time-Aware Inverse Kinematics for Dual-Arm Systems

\*Yucheng Tang<sup>1,2,3</sup>, \*Xi Huang<sup>3</sup>, Yongzhou Zhang<sup>1,3</sup>, Tao Chen<sup>2,3</sup>, Ilshat Mamaev<sup>1,2</sup>, Björn Hein<sup>1,3</sup>

**Abstract**—This paper presents ETA-IK, a novel Execution-Time-Aware Inverse Kinematics method tailored for dual-arm robotic systems. The primary goal is to optimize motion execution time by leveraging the redundancy of both arms, specifically in tasks where only the relative pose of the robots is constrained, such as dual-arm scanning of unknown objects. Unlike traditional inverse kinematics methods that use surrogate metrics such as joint configuration distance, our method incorporates direct motion execution time and implicit collisions into the optimization process, thereby finding target joints that allow subsequent trajectory generation to get more efficient and collision-free motion. A neural network based execution time approximator is employed to predict time-efficient joint configurations while accounting for potential collisions. Through experimental evaluation on a system composed of a UR5 and a KUKA iiwa robot, we demonstrate significant reductions in execution time. The proposed method outperforms conventional approaches, showing improved motion efficiency without sacrificing positioning accuracy. These results highlight the potential of ETA-IK to improve the performance of dual-arm systems in applications, where efficiency and safety are paramount.

## I. INTRODUCTION

While robots are becoming increasingly capable of performing everyday tasks in a Human-Robot Collaboration setting, there are still many situations where robots must operate without humans present in the environment. Notable examples include dismantling nuclear facilities, disaster relief operations, and tasks in human-hazardous environments [1] [2]. In such environments, the criteria of human likeness and the predictability of motion, which are essential for collaborative tasks, are of less importance than efficiency, which represents the gold standard.

Our work originates from a scenario involving the scanning and modeling of unknown objects during the dismantling and decontamination of a nuclear facility. To be specific, robots have to efficiently coordinate with each other to conduct rapid surface modeling and reconstruction of a unknown object. With the sophisticated reconstructed 3D model, a close-range radiation scanning over the surface of the unknown object is then possible. The focus of this work is the motion generation for rapid modeling. For the modeling

This paper is the scientific result of a research project "ROBDEKON2", funded by the German Federal Ministry of Education and Research (BMBF), Grant No. 13N16543.

<sup>1</sup>The authors are with the Karlsruhe University of Applied Sciences, Karlsruhe, Germany {yucheng.tang, ilshat.mamaev, christian.wurll, bjoern.hein}@h-ka.de

<sup>2</sup>The authors are with Proximity Robotics & Automation GmbH, {tang, mamaev}@proximityrobotics.com

<sup>3</sup>Karlsruhe Institute of Technology, Karlsruhe, Germany

\*These authors contributed equally to this work

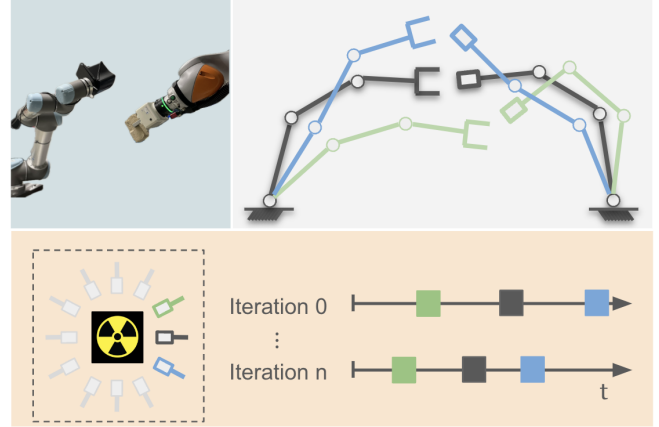


Fig. 1: Improving execution time for modeling radioactive unknown objects with two robot arms (top left). Given a set of relative poses representing the scan poses (bottom left), ETA-IK aims to use the capabilities of this highly redundant system to solve the IK problem and find the optimal and collision-free joint configurations (top right), to accelerate the scanning process (bottom right).

task, the robots traverse over a given sequence of object-centric perception angles, e.g. generated from Next-Best-View (NBV) methods [3] [4]. At least one robot should manipulate and then hold the object for perception while another robot with perception instruments attached should position itself to approach the predefined perception angle, i.e. to keep a relative pose including position and orientation to the first robot. As the perception completes, the both robots move on to the next perception angles in the sequence. Note that the perception angles, i.e. the relative pose between the robots, only imposes a constraint of six Degrees of Freedom (DoF), leaving us possibility to leverage redundancy of the robot arms to optimize the joint configurations for higher efficiency, e.g. shorter time traversing from one perception pose to the next one in the given sequence.

In this work, we use the motion execution time traversing from the current robot configuration to the target pose as a metric to characterize the efficiency. The goal of the this work is to compute the target joint configurations that can reach the target pose while keeping the execution time as short as possible. This metric can be integrated into a multi-objective inverse kinematics framework. Some inverse kinematics algorithms use difference between joint configurations as surrogate loss [5] [6]. This surrogate loss becomes less representative if the point-to-point motion from the current

robot joint configuration to the computed target configuration is not collision-free. This is a common phenomenon in the dual-arm setting. On the other hand, we use a learned neural network to directly provide an estimation of the motion execution time, taking into account the detour to avoid collision, resulting in a more accurate and representative metric. The main contributions of this work are as follows,

- A multi-objective Inverse Kinematics (IK) method for dual-arm setting that formulates the problem using relative pose between TCPs of the robots, optimizing simultaneously over the redundancy of both arms
- Improving motion execution efficiency by directly including motion execution time into the IK optimization problem, showing significant advantage compared to the methods that use surrogate terms such as joint distance
- An execution time approximator that takes into account potential risks of collision, providing more accurate estimation regarding execution time of a collision-free point-to-point motion generated by standard Trajectory Generation (TG) given the the start and target configurations

## II. RELATED WORK

*Explore Redundancy Resolution for Redundant Robot and Dual-arm System:* Redundant robots are robotic systems that have more DoF than is strictly necessary to perform a given task, and for regular reach a pose tasks, robots with more than six DoF have redundancy. Numerous studies have leveraged redundancy resolution in seven DoF robots to enhance motion optimization, such as introducing joint limit constraints [7], improving manipulability to avoid singularities [8], enhancing stiffness [9], avoiding obstacles [10], or reducing energy consumption [11]. When the objective is to achieve coordinated relative poses between multiple robotic arms, the nullspace of the relative Jacobian becomes larger, enabling further optimization across multiple sub-tasks or asymmetric tasks [12] [13].

Some research has extended the concept of the nullspace by incorporating advanced optimization strategies. For instance, cost functions based on the manipulability of key waypoints have been proposed to define secondary tasks [14], thereby optimizing the average manipulability index throughout the task execution. Additionally, by deriving the nullspace into acceleration domain, nullspace-based impedance controller is proposed to handle force interactive tasks [15] and minimization of motion time under kinematic/dynamic bounds can also be achieved [16].

To the best of the author's knowledge, there is currently no research that directly incorporates execution time explicitly into the IK optimization problem. Some studies [5] [6] that aim to find a global optimum introduce a distance cost function specific to the joint configuration. By setting a specific angle as the current joint configuration, these methods attempt to minimize joint movements, thereby optimizing execution time. However, achieving a global optimum requires converting the optimization problem into a convex form, which restricts the extensibility of objective function and

leads to an exponential increase in computational time as the number of redundant degrees of freedom increases. In addition, other related methods include inertial load optimization based on Cartesian spatial direction and the concepts of pseudo-inverse velocity and pseudo-inverse acceleration [16]. These methods are more suitable for local optimization and path following, which differs from the problem addressed in this work.

*Time-Optimal Trajectory Generation:* Traditional methods to optimize the execution time are usually incorporated into the trajectory optimization step, after IK solving and path planning. There are many approaches, such as Time Scaling, Time-Optimal Path Parameterization (TOPP) [17], Time-Optimal Path Parameterization Based on Reachability Analysis (TOPPRA) [18], and other Time-Optimal Trajectory Generation (TOTG) techniques [19] [20], are typically applied as post-processing steps rather than being integrated into the single-pose IK solution. While these methods are capable of generating efficient motions, they generally assume that a feasible joint target pose or a series of waypoints is already available. This makes them more appropriate for waypoint-based motion planning, as opposed to addressing single-pose IK challenges.

*Learning-based Approaches:* Regarding the learning based IK solver, very earlier, the authors in [21] proposed to use a prediction network to reduce the IK solving time. Numerous studies [22] [23] [24] have explored various neural network architectures for solving the IK problem.

Directly learning an IK solution for redundant robots using an end-to-end neural network approach presents significant challenges. IKNET [25] demonstrated improvements compared to MLP by decreasing the position error into the centimeter level. Unsupervised learning-based IK is proposed for highly redundant system [26], reducing the error of a 20 DoF redundant robot to 2 cm when only the position error is considered. Another important finding is that the neural network solver is capable of implicitly generating collision-free solutions when trained on datasets containing obstacle avoidance scenarios. On the other hand, for the IK solver based on optimization, the network can be used to estimate some metrics, such as the nullspace parameter [27]. For a dual-arm robotic system with 12 to 14 DoFs, integrating learning-based methods with optimization has the potential to address the limitations of both approaches.

## III. PROBLEM STATEMENT

The primary goal of this work was to find a target joint configuration  $\mathbf{q}_t$  for a point-to-point (PTP) minimum motion time IK problem with a given initial configuration  $\mathbf{q}_0$ , a desired target Tool Center Point (TCP) pose  $\mathbf{p}_t$  (relative pose between 2 TCPs  $\mathbf{p}_{r,t}$  for a dual-arm system), zero initial/final joint velocity  $\dot{\mathbf{q}}_0 = \dot{\mathbf{q}}_t = 0$ , and robot dynamic and kinematic limits as follow:

$$\begin{aligned} \mathbf{q}_{\min} &\leq \mathbf{q}(t) \leq \mathbf{q}_{\max}, \\ \dot{\mathbf{q}}_{\min} &\leq \dot{\mathbf{q}}(t) \leq \dot{\mathbf{q}}_{\max}, \\ \ddot{\mathbf{q}}_{\min} &\leq \ddot{\mathbf{q}}(t) \leq \ddot{\mathbf{q}}_{\max} \quad \forall t \in [0, t_{\text{end}}]. \end{aligned} \quad (1)$$

The primary motivation for formulating this problem is to optimize the process of scanning unknown objects as efficiently as possible using the NBV method. In a dual-arm robotic system, where one arm holds the unknown object and the other is equipped with a scanner or camera, the NBV is defined by the relative pose of the two TCPs. Given the redundancy of the robotic system, there exists an infinite number of configurations that can satisfy the relative pose constraints. To identify the most efficient IK solution for this motion task, the distance between the initial and target configurations can serve as a potential metric for estimating motion time. However, this approach is complicated by the fact that most robots have unique joint limits, making it challenging to predict motion time based solely on configuration distance. And the estimated joint distance in the IK phase can not explicitly illustrate the actual execution time due to the collision avoidance behaviour considered in the post-processing phase.

As mentioned above, most time-optimization methods for motion execution apply post-processing to target configurations or joint waypoints after they are determined. It remains an open question regarding how to explore the solution space of a single inverse kinematics (IK) problem to obtain a configuration that optimizes execution time directly. The closest approach mentioned in [16] models the problem as a nonlinear programming problem and employs numerical methods based on direct collocation to minimize execution time. While this approach calculates the optimal trajectory simultaneously with the execution time, it introduces significant computational overhead.

#### IV. APPROACH

With the six DoF perception poses generated by the NBV algorithms, we leverage redundancy of the dual arms to optimize the joint configurations for fast execution. First, we use the relative pose between both arms to formulate an inverse kinematics problem. Then, we convert this formulation into a parallel multi-objectives problem and incorporate execution time directly in the objectives. During the optimization, the joint configurations converge to the target desired pose and sequentially improve the execution time.

##### A. Relative TCP Pose Approach

In a dual-arm robot system, as shown in Fig. 3, one robot, called the tool robot, holds the tool (camera or scanner), while the other arm, called the reference robot, holds the object to be modelled. The concept of relative Jacobian is built on vectors that represent the position and orientation of the TCP of the tool robot relative to the TCP of the reference robot. It imposes a constraint regarding the relative motion between the two TCPs without any restrictions regarding of their absolute positions. Essentially, by using this Jacobian, the focus in a two-arm maneuver is the relative motion between the TCP.

The relative position vector  $\mathbf{x}_R$  is then defined as:

$$\mathbf{x}_R = \mathbf{x}_B - \mathbf{x}_A \quad (2)$$

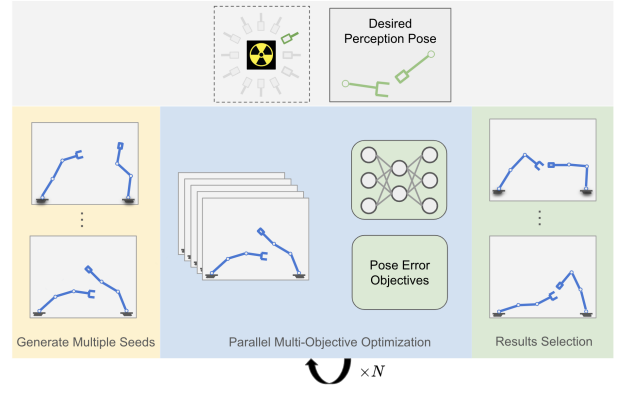


Fig. 2: Pipeline of ETA-IK: given a desired perception pose, ETA-IK first generate a batch of initial configurations, highlighted with yellow. And then, a multilayer-perceptron time approximator and pose error objectives are used for parallel optimization, highlighted with blue. After  $N$  iterations, the results is a batch of joint configurations. We select the best one according to criterion such as execution time and relative pose error between two robots, highlighted with green.

where  $\mathbf{x}_A, \mathbf{x}_B \in \mathbb{R}^{n_R}$  are the TCP pose of the reference robot and the tool robot, respectively and  $n_R$  refers to the DoFs of the robotic arms. By differentiating this equation with respect to time, we obtain:

$$\dot{\mathbf{x}}_R = \dot{\mathbf{x}}_B - \dot{\mathbf{x}}_A = J_R \dot{\mathbf{q}} \quad (3)$$

where  $\dot{\mathbf{x}}_R$  represents the relative velocity between two robots' TCPs and  $\dot{\mathbf{x}}_B, \dot{\mathbf{x}}_A$  denote the absolute velocity of the respective robot's TCP. The relative Jacobian  $J_R \in \mathbb{R}^{n_R \times n_T}$  can be expressed in terms of the individual Jacobians of the robots [15]:

$$J_R = \begin{bmatrix} -R_{RA}J_A \\ R_{RT}^T R_{RB}J_B \end{bmatrix} \quad (4)$$

where  $J_A \in \mathbb{R}^{n_R \times n_A}$  and  $J_B \in \mathbb{R}^{n_R \times n_B}$  are the Jacobians of robots A and B, respectively. The term  $n_{[\cdot]}$  denotes the DoF of a robot and  $n_T = n_A + n_B$  is the total number of DoFs for the system. The block diagonal rotation matrices  $R_{RA}, R_{RT}, R_{RB} \in \mathbb{R}^{n_R \times n_R}$  are determined with respect to their associated reference frames. The relative Jacobian  $J_R$  provide gradients of the pose error in the multi-objective optimization.

##### B. Multi-Objective Relative Pose IK

The primary objective for the defined scenario is to accurately determine the relative pose between the reference robot and the tool robot. To achieve this, the first components of the objective function are defined to address both the relative position and orientation errors.

For the relative position, the objective function can be formulated as:

$$\chi_p(\mathbf{q}) = \|(p_{B,g} - p_{A,g}) - (FK_B(\mathbf{q}_B) - FK_A(\mathbf{q}_A))\|^2 \quad (5)$$

where  $FK_A(\mathbf{q}_A)$  and  $FK_B(\mathbf{q}_B)$  are the forward kinematics functions of robots A and B given their joint configurations.

For the relative orientation error, the objective function is given by:

$$\chi_o(\mathbf{q}) = d(d(q_{B,g}, q_{A,g}), d(q_B[FK(\mathbf{q}_B)], q_A[FK(\mathbf{q}_A)])), \quad (6)$$

where  $d(\cdot)$  is the displacement between two quaternions, and note that  $\mathbf{q}$  refers joint configuration of the robot, and  $q$  represents quaternions.

To represent the motion time, a commonly used surrogate metric is the distance between the starting and target joint configurations:

$$\chi_{mt}(\mathbf{q}) = \|\mathbf{q} - \mathbf{q}_0\|^2, \quad (7)$$

where  $\mathbf{q}$  is the joint configuration being optimized. In this formulation, a bang-bang control strategy can be assumed at the velocity level, and the distance metric is normalized by introducing a weighting factor to account for the different velocity limits of each joint.

$$\chi_{mt}(\mathbf{q}) = \sum_{i=1}^{n_T} w_i |q_i - q_{i,0}|^2. \quad (8)$$

### C. Optimization

Inverse kinematics optimization aiming for global optimality is significant computationally expensive. Recent study [6] reports an average computation time of 77.6 seconds to optimize a system with 10 DoF using the similar objective functions in IV-B. The optimizing problems of a dual-arm system involves commonly 12-14 DoF, resulting in an expanded optimization space. Due to the curse of dimensionality, this increase significantly elevates computational expense, rendering such methods impractical.

The other non-convex optimization algorithms such as [28], trade global optimality for potentially faster computation. To improve the chances of finding a better solution, a parallel optimization approach is often employed [29]. This method uses multiple initial guesses in parallel, and the best result is selected as the optimal solution. Since the mapping relationship between Cartesian coordinates and the joints of a redundant manipulator is not unique, the number and distribution of initial guesses can significantly influence the final optimization result.

The entire objective function is

$$f(\mathbf{q}) = w_p \cdot \chi_p(\mathbf{q}) + w_o \cdot \chi_o(\mathbf{q}) + w_m t \cdot \chi_{mt}(\mathbf{q}, \mathbf{q}_0) + w_b \cdot \chi_b(\mathbf{q}) \quad (9)$$

where  $w_i$  represent the weight for the corresponding objective terms, and  $\chi_b(\mathbf{q})$  is the joint limit cost proposed in [29]. Initially, Halton sampling is employed to generate samples from the configuration space that are free of collisions, serving as initial guesses for the optimization process. The step directions for the optimization are then computed based on the gradient of the defined objective function.

Once the step direction is determined, a line search is conducted. This involves scaling the step direction with a discrete set of magnitudes [29]. The optimal magnitude from this set is selected using the Armijo and Wolfe conditions, ensuring that the step size is sufficient for descent

and satisfies the curvature condition, which is crucial for avoiding overshooting and ensuring stable convergence in IK problems.

After several iterations, all optimization results are verified for feasibility and convergence to ensure that the calculated IK solutions reside in a collision-free joint space and meet the predefined position and rotation error thresholds. A solution is considered successful if it satisfies both conditions. If a solution does not meet these criteria, an offset is added to the evaluation metric when selecting the best solution.

Typically, the IK problem defines the optimal solution as the one that minimizes the pose error. Since our method also consider the motion time, the metric for selecting the optimal solution can be defined in several ways: it can prioritize the pose error, the motion time, or a combination of both. This flexibility allows the optimization to balance accuracy in achieving the desired pose with the efficiency of motion, depending on the specific requirements of the task.

### D. Execution Time Approximator

Using surrogate loss such as distance between joint configurations as optimization objectives assumes that resultant point-to-point motion between the start and target configuration is collision-free and executable. For a dual-arm setting, this assumption is usually not legitimate and therefore a post-processing step such as path planning is needed. This additional step introduce an gap between the surrogate loss and the actual execution time. Directly coping execution time in the optimization does not has such problem.

For dual arms mounted on a fixed base, we can deploy offline optimal path planning or trajectory optimization algorithms to compute the collision-free motion between two arbitrary joint configuration and at the end acquire the actual execution time. However, this paradigm can not be included into the multi-objective optimization due to its computation complexity. Instead, we collect data from these offline methods and use a multilayer perceptron (MLP)  $f_\theta$  to approximate the execution time during the optimization. Previous works [30] show that MLPs are capable to capture the latent relation between joint configurations and time. Furthermore, MLPs can not only achieve fast inference time during optimization, but also support batch operations and provide gradients for the optimization. In practice, we use positional encoding  $\mathbf{q}_{PE} = [\mathbf{q}, \cos \mathbf{q}, \sin \mathbf{q}]$  as input for the approximator. Given the start and target configuration  $\mathbf{q}_0, \mathbf{q}_t$ , the approximator outputs

$$\hat{t} = f_\theta(\mathbf{q}_{PE,0}, \mathbf{q}_{PE,t}). \quad (10)$$

Literature [31] [32] suggests that this can improve the expressiveness of the MLP.

## V. EXPERIMENTAL EVALUATIONS

The experimental setup for the dual-arm system, shown in 3, consists of a UR5 and a KUKA LBR iiwa 14 R820 robot, with a combined total of 13 DoF. The KUKA iiwa is designated for object grasping due to its higher load capacity, while a high-resolution 3D lidar Robin W from Seyond is mounted on the UR5's end-effector for scanning purposes.

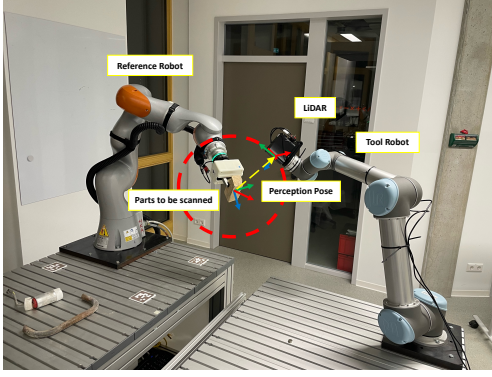


Fig. 3: **Scanning and modeling with two different manipulators:** The KUKA iiwa robot picks up the target object (stone) and the UR5 robot carries a 3D lidar scanner. To get a complete and accurate model, both robots have to change the scanning pose through many relative poses that are projected as the best scanning perspective. This process needs to be accelerated by using our proposed approach.

#### A. Training Dataset

Given a start and target configuration, the time approximator provides an estimated execution time with implicit consideration of potential collision risk. To train the time approximator, we generate 250,000 collision-free start and target pairs. Then, we feed these pairs to the TOPPRA [18] trajectory generator and Curobo TrajOpt [29] to collect respective execution time. The difference between these two trajectory generators is that, the one from Curobo takes collision into account and always returns collision-free trajectories while the TG methods can return trajectories that are not executable. In our generated dataset, approximately 50% of the trajectories generated by TOPPRA are not collision-free and, therefore, not executable in practice.

#### B. Simulation

1) *Evaluation Simulation Setup:* In the simulation, a general evaluation of the proposed approach is conducted. This involves generating a random collision-free initial joint configuration  $\mathbf{q}_0$  and a random relative Cartesian pose  $\mathbf{p}_{R,t}$ . A random reference target joint configuration  $\mathbf{q}_t$  is sampled, and the absolute TCP poses of the two robots are then calculated individually.

For comparative analysis, three baselines are provided. These baselines utilize the random reference  $\mathbf{q}_t$  directly as the endpoint, perform optimization on Eq. (8) based on absolute and relative Cartesian pose as motion time term in the objective function. The resulting motion time based on the IK solutions is subsequently calculated using the TOPPRA algorithm.

The robot joint limits used when generating the dataset for the network align with those in TOPPRA, including velocity  $\{3.15, 3.15, 3.15, 3.2, 3.2, 3.2\}$  and  $\{10.0, 10.0, 10.0, 10.0, 10.0, 10.0\} \frac{rad}{s}$ , acceleration  $\{5.0, 5.0, 3.0, 2.0, 2.0, 2.0\}$ ,  $\{5.0, 5.0, 3.0, 2.0, 2.0, 2.0\} \frac{rad}{s^2}$ , and jerk constraints for UR5 and IIWA

respectively  $\{500.0, 500.0, 500.0, 500.0, 500.0, 500.0\}$ ,  $\{500.0, 500.0, 500.0, 500.0, 500.0, 500.0\} \frac{rad}{s^3}$ . All optimization parameters are summarized in Tab. I. To explore the optimal solution, the number of initial guesses and optimization iterations are set to a high value, namely 4096 initial guesses and 500 iterations. This ensures a comprehensive evaluation of the solution space. The weights for position and orientation error are 2000, 2500 and the execution time weights are set as 250, 500 for joint distance and execution time approximator, respectively.

2) *Execution Time Evaluation:* The execution time results indicate that using absolute Cartesian coordinates as position targets is less effective than relative positions for execution time optimization. The distance loss (C in the Tab. I) and the proposed execution time approximator with cost based IK solution selection (E) demonstrate comparable performance in optimizing the execution time. It is worth noting that due to the greater optimization space, the positional error of (E) is significantly smaller. If the solution to success is sorted only by execution time cost, the solution obtained by proposed ETA-IK is almost 25% shorter than the execution time of the randomly generated ref configuration, performs best among all comparison methods.

3) *Implicit Collision Consideration:* For the approximator trained by the collision-free dataset, the NBV candidate poses are utilized as target relative poses. Since these scanned positions are object-centered, they are more prone to collisions, thereby highlighting the influence of the collision-aware approximator on the IK solution. As shown in the Tab. II, the trained approximator demonstrates faster performance in both TG methods, with and without collision checking. Method (C), which employs relative position and distance loss as objectives, results in minimal joint changes (A typical example with random sampled starting and target is shown in Fig. 4). However, due to the need for collision avoidance, the final collision-free trajectory execution time is longer than method (G). The symmetry of the velocity profile indicates the presence of obstacle avoidance behavior. While the reference trajectory is planned without encountering obstacles, resulting in a completely symmetrical velocity profile. The longer joint movement distances increased the execution time. In contrast, the IK solution obtained through the proposed approximator optimization exhibits relatively less obstacle avoidance behavior and achieves optimal execution time among the three methods considered.

#### C. Real Robot Experiments

The real robot experiments validated the motion generation pipeline, demonstrating that the generated trajectories perform effectively both in the simulation environment and on real robots. A video of the experiment is attached to provide a visual demonstration of the system's performance.

## VI. DISCUSSION AND CONCLUSION

In this work, we presented ETA-IK, an Execution-Time-Aware Inverse Kinematics method for dual-arm systems,



Metrics	Ref. $q_t$	(A)	(B)	(C)	(D)	(E)	(F)
execution time by TOPPRA	2.71	2.618	2.363	2.477	<b>2.053</b>	2.450	2.807
Position error	0	0.0004	0.0002	0.0022	0.0016	0.0003	0.0003
IK success rate	-	100	100	98	100	100	100

TABLE I: Resulting execution time with random sampling from 100 IK instances (A) Given TCP-pose with distance loss (B) Given TCP-pose with trained model and best time selection (C) Relative pose with distance loss (D) relative pose with trained model and best time selection (E) relative pose with trained model and best cost selection (F) relative pose with trained model and best pose error

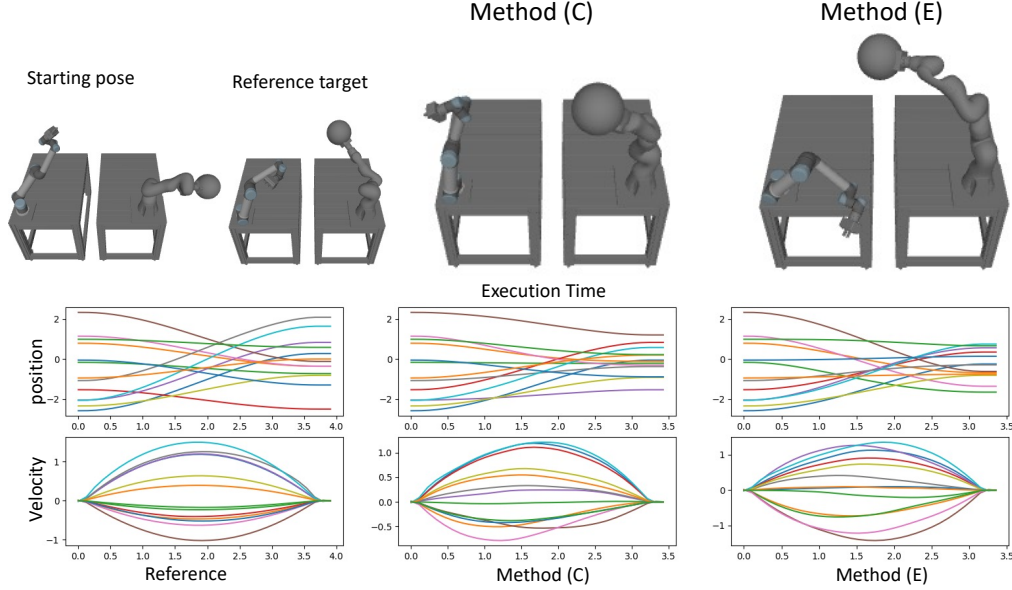


Fig. 4: **Execution time comparison between reference, method (C) and (G) for collision-free trajectory generation:** The starting pose and the reference target shown are randomly generated. The starting joint configuration, reference target configuration, and the IK solution generated by method (C) and (G) in Tab. II are illustrated with the corresponding position and velocity profile over time generated by TrajOpt.

Metrics	Ref. $q_t$	(C)	(G)
execution time by TOPPRA	2.483	2.4529	<b>2.394</b>
execution time by TrajOpt	3.522	3.513	<b>3.40</b>
position error	0	0.0016	0.002
IK success rate	-	100	100

TABLE II: Resulting execution time with task related relative pose from 100 IK instances (C) Relative pose with distance loss (G) relative pose with trained collision-free model

with a specific application in scanning unknown objects during the dismantling of a nuclear facility. Our primary focus was on optimizing motion execution time by leveraging the redundancy of dual-arm systems. The results demonstrated that integrating motion execution time directly into the IK optimization framework yields significant improvements in efficiency compared to traditional methods that rely on surrogate metrics, such as joint distance.

The experiments showed that our proposed execution time approximator effectively improves the overall system performance. By incorporating collision avoidance into the optimization process, our approach could account for self-

collision without introducing substantial computational overhead. This was particularly evident in both simulated and real-world scenarios, where the system was able to achieve more efficient execution while maintaining the relative pose between the two robots.

In addition, we have identified several limitations in this work. One is the additional inference time required for the neural network-based approximator compared to simple distance-based metrics. However, this drawback is mitigated by the overall improvement in the motion execution time. Future work could focus on reducing the computational overhead of the approximator and exploring the application of this approach to multi-robot systems with higher degrees of freedom.

## REFERENCES

- [1] P. Woock, J. Peterit, C. Frey, and J. Beyerer, "ROBDEKON – competence center for decontamination robotics," *at - Automatisierungstechnik*, vol. 70, no. 10, pp. 827–837, Oct. 2022, publisher: De Gruyter (O). [Online]. Available: <https://www.degruyter.com/document/doi/10.1515/auto-2022-0072/html>
- [2] J. Peterit, J. Beyerer, T. Asfour, S. Gentes, B. Hein, U. D. Hanebeck, F. Kirchner, R. Dillmann, H. H. Götting, M. Weiser, M. Gustmann, and T. Eglloffstein, "ROBDEKON: Robotic Systems for Decontamination

- in Hazardous Environments,” in *2019 IEEE International Symposium on Safety, Security, and Rescue Robotics (SSRR)*, Sep. 2019, pp. 249–255, iSSN: 2475-8426. [Online]. Available: <https://ieeexplore.ieee.org/document/8848969/?arnumber=8848969>
- [3] S. Pan, H. Hu, and H. Wei, “SCVP: Learning One-Shot View Planning via Set Covering for Unknown Object Reconstruction,” *IEEE Robotics and Automation Letters*, vol. 7, no. 2, pp. 1463–1470, Apr. 2022. [Online]. Available: <https://ieeexplore.ieee.org/document/9670705/>
  - [4] S. Kobayashi, W. Wan, T. Kiyokawa, K. Koyama, and K. Harada, “Obtaining an Object’s 3D Model Using Dual-Arm Robotic Manipulation and Stationary Depth Sensing,” *IEEE Transactions on Automation Science and Engineering*, vol. 20, no. 3, pp. 2075–2087, Jul. 2023, conference Name: IEEE Transactions on Automation Science and Engineering. [Online]. Available: <https://ieeexplore.ieee.org/document/9849487/?arnumber=9849487>
  - [5] P. Trutman, M. S. E. Din, D. Henrion, and T. Pajdla, “Globally Optimal Solution to Inverse Kinematics of 7DOF Serial Manipulator,” *IEEE Robotics and Automation Letters*, vol. 7, no. 3, pp. 6012–6019, Jul. 2022, conference Name: IEEE Robotics and Automation Letters. [Online]. Available: <https://ieeexplore.ieee.org/document/9745328/?arnumber=9745328>
  - [6] T. Votrubeck and T. Kroupa, “Globally Optimal Inverse Kinematics as a Quadratic Program,” Apr. 2024, arXiv:2312.15569 [cs]. [Online]. Available: <http://arxiv.org/abs/2312.15569>
  - [7] F. Flacco, A. De Luca, and O. Khatib, “Motion control of redundant robots under joint constraints: Saturation in the Null Space,” in *2012 IEEE International Conference on Robotics and Automation*, May 2012, pp. 285–292, iSSN: 1050-4729. [Online]. Available: <https://ieeexplore.ieee.org/document/6225376>
  - [8] N. Vahrenkamp and T. Asfour, “Representing the robot’s workspace through constrained manipulability analysis,” *Autonomous Robots*, vol. 38, no. 1, pp. 17–30, Jan. 2015. [Online]. Available: <https://doi.org/10.1007/s10514-014-9394-z>
  - [9] Y. Tang, W. Shen, I. Mamaev, and B. Hein, “Towards Flexible Manufacturing: Motion Generation Concept for Coupled Multi-Robot Systems,” in *2023 IEEE 19th International Conference on Automation Science and Engineering (CASE)*, Aug. 2023, pp. 1–7, iSSN: 2161-8089. [Online]. Available: <https://ieeexplore.ieee.org/document/10260365/?arnumber=10260365>
  - [10] Y. Jiang, C. Yang, Z. Ju, and J. Liu, “Obstacle Avoidance of a Redundant Robot Using Virtual Force Field and Null Space Projection,” in *Intelligent Robotics and Applications*, H. Yu, J. Liu, L. Liu, Z. Ju, Y. Liu, and D. Zhou, Eds. Cham: Springer International Publishing, 2019, pp. 728–739.
  - [11] A. Dietrich, C. Ott, and A. Albu-Schäffer, “An overview of null space projections for redundant, torque-controlled robots,” *The International Journal of Robotics Research*, vol. 34, no. 11, pp. 1385–1400, Sep. 2015. [Online]. Available: <http://journals.sagepub.com/doi/10.1177/0278364914566516>
  - [12] H. Su, S. Li, J. Manivannan, L. Bascetta, G. Ferrigno, and E. D. Momi, “Manipulability Optimization Control of a Serial Redundant Robot for Robot-assisted Minimally Invasive Surgery,” in *2019 International Conference on Robotics and Automation (ICRA)*, May 2019, pp. 1323–1328, iSSN: 2577-087X. [Online]. Available: <https://ieeexplore.ieee.org/document/8793676/?arnumber=8793676>
  - [13] S. Tarbouriech, B. Navarro, P. Fraisse, A. Crosnier, A. Cherubini, and D. Sallé, “Dual-arm relative tasks performance using sparse kinematic control,” in *IROS: Intelligent Robots and Systems*, ser. Towards a Robotic Society, Madrid, Spain, Oct. 2018, pp. 6003–6008. [Online]. Available: <https://hal.science/hal-01735462>
  - [14] M. Faroni, M. Beschi, A. Visioli, and L. Molinari Tosatti, “A global approach to manipulability optimisation for a dual-arm manipulator,” in *2016 IEEE 21st International Conference on Emerging Technologies and Factory Automation (ETFA)*, Sep. 2016, pp. 1–6. [Online]. Available: <https://ieeexplore.ieee.org/document/7733725/>
  - [15] J. Lee, P. Chang, and R. Jamisola, “Relative Impedance Control for Dual-Arm Robots Performing Asymmetric Bimanual Tasks,” *IEEE Transactions on Industrial Electronics*, vol. 61, pp. 3786–3796, Jul. 2014.
  - [16] K. Al Khudir and A. De Luca, “Faster Motion on Cartesian Paths Exploiting Robot Redundancy at the Acceleration Level,” *IEEE Robotics and Automation Letters*, vol. 3, no. 4, pp. 3553–3560, Oct. 2018, conference Name: IEEE Robotics and Automation Letters. [Online]. Available: <https://ieeexplore.ieee.org/document/8408564/?arnumber=8408564>
  - [17] Q.-C. Pham, “A General, Fast, and Robust Implementation of the Time-Optimal Path Parameterization Algorithm,” *IEEE Transactions on Robotics*, vol. 30, no. 6, pp. 1533–1540, Dec. 2014, arXiv:1312.6533 [cs]. [Online]. Available: <http://arxiv.org/abs/1312.6533>
  - [18] H. Pham and Q.-C. Pham, “A New Approach to Time-Optimal Path Parameterization based on Reachability Analysis,” Nov. 2017, arXiv:1707.07239 [cs]. [Online]. Available: <http://arxiv.org/abs/1707.07239>
  - [19] L. Berscheid and T. Kröger, “Jerk-limited Real-time Trajectory Generation with Arbitrary Target States,” arXiv:2105.04830 [cs], Jun. 2021, arXiv: 2105.04830. [Online]. Available: <http://arxiv.org/abs/2105.04830>
  - [20] T. Kröger, “Opening the door to new sensor-based robot applications—The Reflexxes Motion Libraries,” in *2011 IEEE International Conference on Robotics and Automation*, May 2011, pp. 1–4, iSSN: 1050-4729.
  - [21] E. Oyama, N. Y. Chong, A. Agah, and T. Maeda, “Inverse kinematics learning by modular architecture neural networks with performance prediction networks,” in *Proceedings 2001 ICRA. IEEE International Conference on Robotics and Automation (Cat. No. 01CH37164)*, vol. 1. IEEE, 2001, pp. 1006–1012.
  - [22] M. N. Vu, F. Beck, M. Schwegel, C. Hartl-Nesic, A. Nguyen, and A. Kugi, “Machine learning-based framework for optimally solving the analytical inverse kinematics for redundant manipulators,” *Mechatronics*, vol. 91, p. 102970, 2023.
  - [23] B. Bócsi, D. Nguyen-Tuong, L. Csató, B. Schoelkopf, and J. Peters, “Learning inverse kinematics with structured prediction,” in *2011 IEEE/RSJ International Conference on Intelligent Robots and Systems*. IEEE, 2011, pp. 698–703.
  - [24] M. Mahajan and G. C. Nandi, “On Solving Inverse Kinematics of Redundant Robots Using Invertible Neural Networks with Ex-Post Density Estimation.”
  - [25] R. Bensadoun, S. Gur, N. Blau, T. Shenkar, and L. Wolf, “Neural Inverse Kinematics,” May 2022, arXiv:2205.10837 [cs]. [Online]. Available: <http://arxiv.org/abs/2205.10837>
  - [26] B. Stephan, I. Dontsov, S. Müller, and H.-M. Gross, “On Learning of Inverse Kinematics for Highly Redundant Robots with Neural Networks,” in *2023 21st International Conference on Advanced Robotics (ICAR)*. Abu Dhabi, United Arab Emirates: IEEE, Dec. 2023, pp. 402–408. [Online]. Available: <https://ieeexplore.ieee.org/document/10406939/>
  - [27] C. Towell, M. Howard, and S. Vijayakumar, “Learning nullspace policies,” in *2010 IEEE/RSJ International Conference on Intelligent Robots and Systems*. Taipei: IEEE, Oct. 2010, pp. 241–248. [Online]. Available: <http://ieeexplore.ieee.org/document/5650663/>
  - [28] D. Rakita, B. Mutlu, and M. Gleicher, “RelaxedIK: Real-time Synthesis of Accurate and Feasible Robot Arm Motion,” in *Robotics: Science and Systems XIV*. Robotics: Science and Systems Foundation, Jun. 2018. [Online]. Available: <http://www.roboticsproceedings.org/rss14/p43.pdf>
  - [29] B. Sundaralingam, S. K. S. Hari, A. Fishman, C. Garrett, K. Van Wyk, V. Blukis, A. Millane, H. Oleynikova, A. Handa, F. Ramos, N. Ratliff, and D. Fox, “cuRobo: Parallelized Collision-Free Minimum-Jerk Robot Motion Generation,” Nov. 2023, arXiv:2310.17274 [cs]. [Online]. Available: <http://arxiv.org/abs/2310.17274>
  - [30] X. Huang, G. Soti, C. Ledermann, B. Hein, and T. Kröger, “Planning with learned subgoals selected by temporal information,” in *2024 IEEE International Conference on Robotics and Automation (ICRA)*. IEEE, 2024, pp. 9306–9312.
  - [31] M. Koptev, N. Figueroa, and A. Billard, “Neural joint space implicit signed distance functions for reactive robot manipulator control,” *IEEE Robotics and Automation Letters*, vol. 8, no. 2, pp. 480–487, 2022.
  - [32] B. Mildenhall, P. P. Srinivasan, M. Tancik, J. T. Barron, R. Ramamoorthi, and R. Ng, “Nerf: Representing scenes as neural radiance fields for view synthesis,” *Communications of the ACM*, vol. 65, no. 1, pp. 99–106, 2021.